

Article

Characterization of a PBAT Degradation Carboxylesterase from *Thermobacillus composti* KWC4

Pan Wu^{1,2,†}, Zhishuai Li^{2,3,4,†} , Jian Gao^{2,4,†}, Yipei Zhao^{1,2} , Hao Wang^{2,3,4}, Huimin Qin¹, Qun Gu^{2,3,4}, Ren Wei^{5,*} , Weidong Liu^{2,3,4,*}  and Xu Han^{2,4,*}

¹ College of Biotechnology, Tianjin University of Science and Technology, No. 9, 13th Avenue, Tianjin Economic and Technological Development Area, Tianjin 300457, China

² Tianjin Institute of Industrial Biotechnology, Chinese Academy of Sciences, 32 West 7th Avenue, Tianjin Airport Economic Area, Tianjin 300308, China

³ University of Chinese Academy of Sciences, 19A Yuquan Road, Beijing 100049, China

⁴ National Technology Innovation Center of Synthetic Biology, 32 West 7th Avenue, Tianjin Airport Economic Area, Tianjin 300308, China

⁵ Junior Research Group Plastic Biodegradation, Institute of Biochemistry, University of Greifswald, Felix-Hausdorf-Str. 8, 17489 Greifswald, Germany

* Correspondence: ren.wei@uni-greifswald.de (R.W.); liu_wd@tib.cas.cn (W.L.); han_x@tib.cas.cn (X.H.)

† These authors contributed equally to this work.

Abstract: The large amount of waste synthetic polyester plastics has complicated waste management and also endangering the environment due to improper littering. In this study, a novel carboxylesterase from *Thermobacillus composti* KWC4 (Tcca) was identified, heterologously expressed in *Escherichia coli*, purified and characterized with various plastic substrates. Irregular grooves were detected on polybutylene adipate terephthalate (PBAT) film by scanning electron microscopy (SEM) after Tcca treatment, and Tcca can also hydrolyze short-chain diester bis(hydroxyethyl) terephthalate (BHET). The optimal pH and temperature for Tcca were 7.0 and 40 °C, respectively. In order to explore its catalytic mechanism and improve its potential for plastic hydrolysis, we modeled the protein structure of Tcca and compared it with its homologous structures, and we identified positions that might be crucial for the binding of substrates. We generated a variety of Tcca variants by mutating these key positions; the variant F325A exhibited a more than 1.4-fold improvement in PBAT hydrolytic activity, and E80A exhibited a more than 4.1-fold increase in BHET activity when compared to the wild type. Tcca and its variants demonstrated future applicability for the recycling of bioplastic waste containing a PBAT fraction.

Keywords: polybutylene adipate terephthalate (PBAT); carboxyl esterase; enzymatic degradation; protein engineering



Citation: Wu, P.; Li, Z.; Gao, J.; Zhao, Y.; Wang, H.; Qin, H.; Gu, Q.; Wei, R.; Liu, W.; Han, X. Characterization of a PBAT Degradation Carboxylesterase from *Thermobacillus composti* KWC4. *Catalysts* **2023**, *13*, 340. <https://doi.org/10.3390/catal13020340>

Academic Editors: Maciej Szaleniec, Bartosz Brzozowski and Marek Adamczak

Received: 21 December 2022

Revised: 20 January 2023

Accepted: 30 January 2023

Published: 3 February 2023



Copyright: © 2023 by the authors. Licensee MDPI, Basel, Switzerland. This article is an open access article distributed under the terms and conditions of the Creative Commons Attribution (CC BY) license (<https://creativecommons.org/licenses/by/4.0/>).

1. Introduction

Biodegradable plastics, such as polybutylene adipate terephthalate (PBAT), maintain some of the beneficial polymer properties of polyester plastics and can be biodegraded at significantly faster rates [1]. They have been introduced to the market as an environmentally friendly alternative to recalcitrant plastics such as polyethylene (PE), and thus they have potential for broader applications [2]. PBAT is a biodegradable aliphatic aromatic co-polyester synthesized by esterifying 1,4-butanediol with an aromatic dicarboxylic acid and then polycondensing with succinic acid [3]. It could be used alone or as a blend component with poly(lactic acid)PLA, PHBV (Poly(β -hydroxybutyrate- β -hydroxyvalerate)), cellulose and many other materials [4–10], and it has been produced on an industrial scale as commercial products, such as mulching films, organic waste bags or packaging material [11]. PBAT can be biodegraded under soil and composting conditions by microorganisms [12–14]; under composting conditions, it can be decomposed within several months [15]. As PBAT

conducted with MEGA11, and the box is Tcca. Carboxylesterase: *Thermobacillus composti* KWC4 (Tcca), WP_015255658.1; *Thermobacillus* sp, REK52384.1; *Thermobifida fusca* (TfCa), WP_104613014.1; *Geobacillus stearothermophilus* (Est55), PDB: 2OGS. Esterase: *Bacillus subtilis*, PDB:1QE3; *Pseudomonas pseudoalcaligenes* (PpEst), WP_003460012; *Clostridium botulinum* (EstA), PDB: 5AH1; *Thermobifida fusca* DSM 43793 (TfH), CAH17554.1. Cutinase: *Humicola insolens* (Hic), PDB: 4OYL; *Thermobifida cellulolytica* (Thc cut1), PDB: 5LUI; *Thermobifida alba* AHK119 (Est119), PDB: 3VIS; *Thermobifida alba* (Est1), D4Q9N1.2. Lipase: *Pelosinus fermentans* (Pfl1), EIW29778.1. Acetylcholinesterase: *Human*, PDB: 4BDT; *Mus musculus*, PDB: 2C0P. Butyrylcholinesterase: *Homo sapiens*, PDB: 6EMI.

Carboxylesterases possess a common catalytic triad consisting of a nucleophile (serine, aspartate, or cysteine), a histidine, and a catalytic acid (aspartate or glutamate) [30]. The serine residue of the catalytic triad is usually found in the pentapeptide G–X–S–X–G, on the nucleophile elbow; these protein share a similar structural fold to the α/β hydrolase superfamily [31]. Among Tcca homologous enzymes with available crystal structures, the following three share the highest protein sequence identities with Tcca: TfCa from *Thermobifida fusca* (PDB: 7W1K [32], 32% identity), Est55 from *Geobacillus stearothermophilus* (PDB: 2OGS [33], 31% identity) and *p*-nitrobenzyl esterase (*p*NB–E) from *Bacillus subtilis* (PDB: 1QE3 [34], 30% identity). Protein sequence alignment of Tcca against TfCa, Est55 and *p*NB–E (Figure 2) indicates that Tcca contains a conserved catalytic triad consisting of S203, E324 and H414, in which S203 is located on the top of “nucleophile elbow” and serves as the nucleophile, to be polarized by the base amino acid H414 and stabilized by the acid amino acid E324 [32–34].

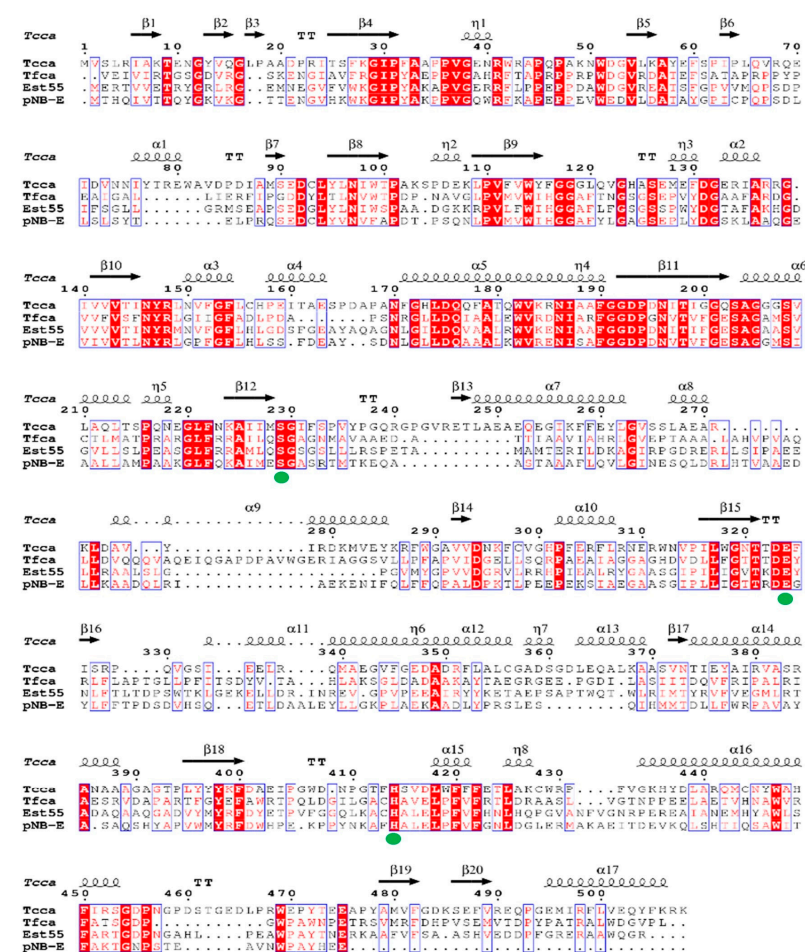


Figure 2. Amino acid sequence alignment of Tcca with homologous enzymes. Alignment of the carboxylesterase sequences used in the consensus analysis. The sequence alignment of Tcca was carried

out with carboxylesterases TfCa from *T. fusca* (PDB: 7W1K), Est55 from *G. stearothermophilus* (PDB: 2OGS), and a pNB-E from *B. subtilis* (PDB: 1QE3). Strictly conserved residues are highlighted in a red background, and catalytic triad consisting residues are represented by green dots. A secondary structure topology based on the structure of Tcca modeling is shown on top of the sequence alignment.

2.2. Characterization of Tcca

Tcca was successfully over-expressed in the *E. coli* BL21 (DE3) and purified to homology using a nickel affinity column. The melting temperatures (T_m), optimum temperature and pH of Tcca were determined using the purified protein (Figure 3). The T_m of Tcca is determined to be 70.07 °C (Figure 3A), suggesting that it has a high thermal stability. The effect of temperature on Tcca activity was explored at various temperatures ranging from 30 to 70 °C, and Tcca exhibited the maximum enzyme activity at 40 °C, but it still retained a 50% relative activity at 30 and 50 °C (Figure 3B). The relative enzyme activity of Tcca was stable in the pH range of 6.0–8.0, with an optimum pH of 7.0 (Figure 3C).

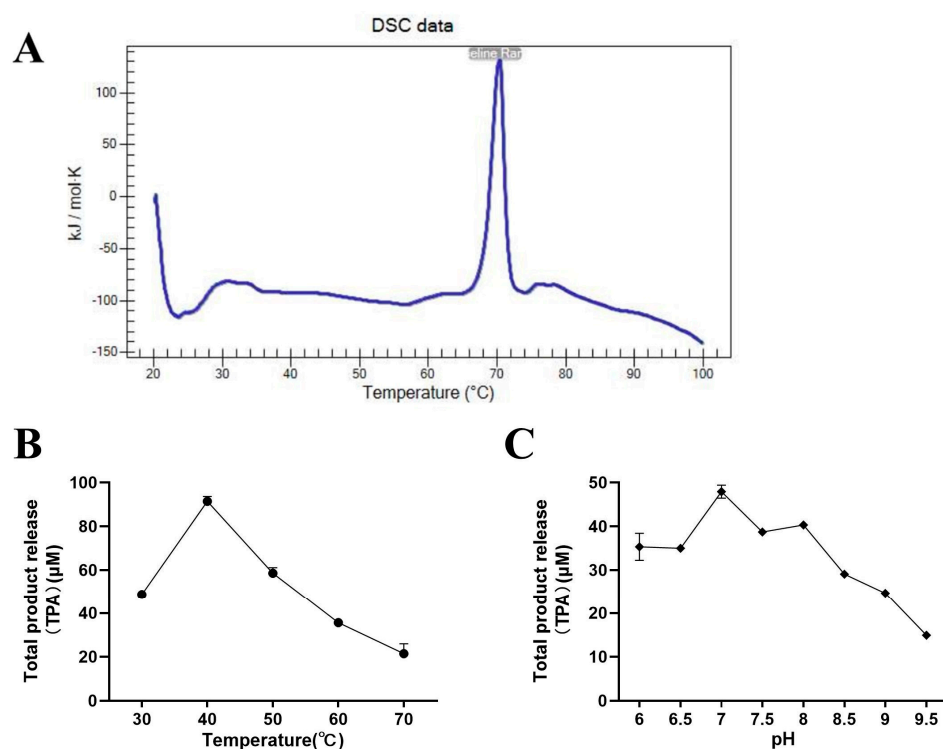


Figure 3. The T_m , optimal pH and temperature of Tcca. (A) The T_m of the Tcca; (B) The optimal temperature of Tcca; (C) The optimal pH of Tcca. The optimum temperature of Tcca was determined to be in the range of 30 to 70 °C, and the optimum pH of Tcca was tested in buffers at pH values ranging from 6.0 to 9.5. All the hydrolysis reactions were performed using a piece of PBAT film (Ø8 mm) with 10.9 μM enzyme in 0.8 mL buffer at 300 rpm for 24 h. Error bars denote the standard deviations calculated based on triplicated determinations.

2.3. The Hydrolysis of PBAT Film by Tcca

The surface modification of PBAT by Tcca was confirmed by scanning electron microscopy (SEM) after a 48h hydrolysis. The buffer-only control sample had a smooth and uniform surface (Figure 4A), and significant modifications with irregular grooves were observed in Tcca-treated samples, indicating that Tcca could degrade PBAT (Figure 4B).

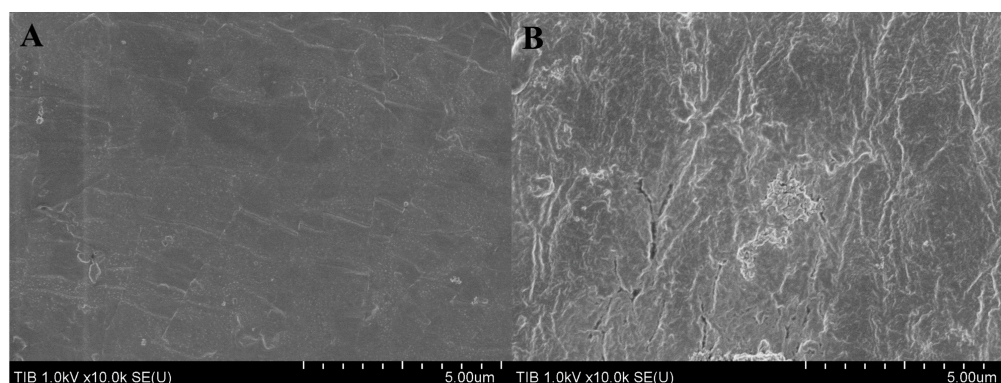


Figure 4. SEM captures of PBAT film surface with and without treatment by Tcca. (A) SEM images (10,000 \times magnification) for control PBAT film without enzymatic treatment; (B) PBAT film after incubation with Tcca. All SEM images were captured after 48 h of incubation at an enzyme loading of 2 mg/mL in 100 mM PBS buffer (pH 8.0) at 40 $^{\circ}$ C or with only buffer as a negative control.

2.4. Tcca Structure Modeling and Possible Substrate Binding Cavity

In order to probe into the possible substrate binding mode of Tcca to its substrates PBAT and BHET (Figure 5A), we modeled the protein structure of Tcca by using AlphaFold [35]. The model exhibits a α/β hydrolase fold comprising a central twisted β -sheet, which is formed by 13 mixed β -strands and surrounded by 16 α -helices (Figure 5B). As observed in other α/β -hydrolases superfamilies [36,37], such as lipases and serine proteases, the catalytic apparatus of carboxylesterase contains three residues: a serine, a glutamate or aspartate, and a histidine. In Tcca, the possible conserved catalytic triad consists of S203–E324–H414 and the conserved serine hydrolase G-x1–S-x2–G motif (G201–Q202–S203–A204–G205). We superimposed the structure of the modeled Tcca with TfCa (PDB: 7W1K) [30], and it turned out that they had very similar overall structures, the main chain root mean square deviation (RMSD) of both structures being 1.230 \AA . The relative positions of the catalytic residues serine, glutamate and histidine, as well as the substrate binding channels, are similar (Figure 5B).

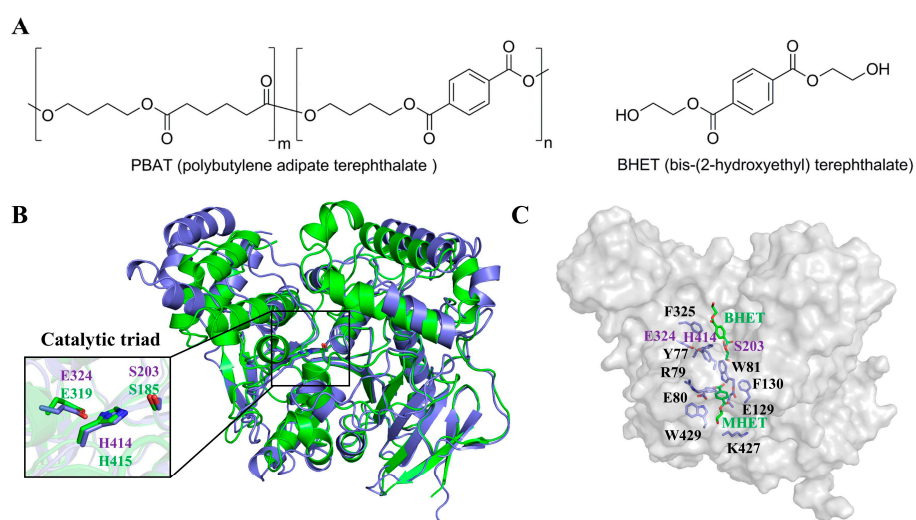


Figure 5. Comparison of Tcca structure and identification of substrate binding tunnel. (A) Illustrations of TCCA substrates PBAT and BHET. (B) Superimposition of modeled Tcca with TfCa crystal structure. The modeled structure of Tcca is in purple, and the crystal structure for TfCa (PDB: 7W1K) is in green. The catalytic triad of Tcca (S203–E324–H414) superimposed well with that of TfCa (S185–E319–H415). (C) Alignment of Tcca to TfCa with bound ligands. The modeled Tcca structure is shown as the surface, the residues around the substrate binding channel of Tcca are shown in sticks in purple, and the bound substrates BHET and MHET are in green.

In recent years, the structural study and protein engineering of plastic degradation enzymes such as PETase have gained a lot of attention. Typically, residues around the substrate binding tunnel are more prone to affect the substrate binding and hydrolytic activity [17]. The complex structure of TfCa with bound mono(2-hydroxyethyl) terephthalate (MHET) and BHET was reported recently, as was its engineering [30]. Similarly, we identified several key residues near the possible substrate binding region of Tcca, and they are Y77, R79, E80, W81, E129, F130, F325, K427 and W429, based on the possible substrate conformation obtained by a structural alignment with TfCa (Figure 5C).

2.5. Protein Engineering of Tcca

In order to check if the aforementioned residues in the substrate binding tunnel of Tcca can affect its activity, we constructed the following variants of Tcca: Y77W, R79A, E80A, W81A, E129A, F130A, F325A, K427A and W429A. All purified variants were evaluated based on their hydrolysis activity in comparison with the wild-type (WT) enzyme against PBAT film and BHET. Tcca and all of its variants exhibited activity on PBAT (Figure 6A). The variant F325A exhibited the highest PBAT hydrolysis activity, which was 1.4-fold higher than the WT enzyme. We hypothesized that switching larger residues to less bulky ones may considerably increase the space in the substrate binding channel, hence increasing the PBAT degradation efficiency. We also examined the activity of these mutants on BHET (Figure 6B). While many of the mutants exhibited clearly decreased BHET hydrolysis activity when compared to the WT enzyme, E80A and F325A showed a 4.1-fold and 2.9-fold increased release of TPA and MHET from BHET after 2 h of incubation, respectively.

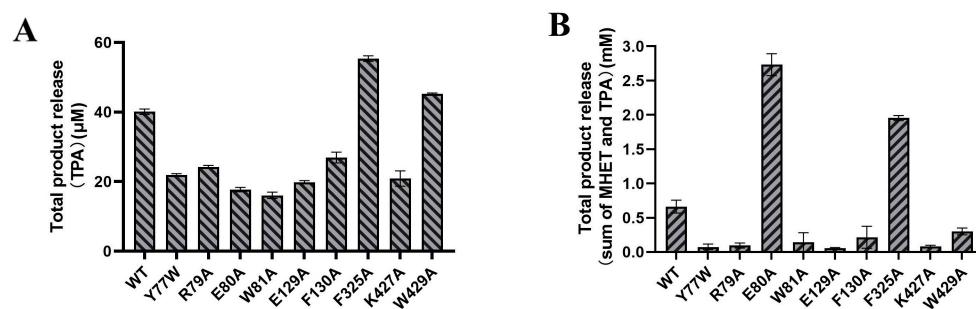


Figure 6. The hydrolysis activity of Tcca and its variants with PBAT and BHET. (A) The amounts of hydrolysis products released after 24 h degradation reaction with PBAT film by Tcca and its variants are shown. (B) The amounts of hydrolysis products released after 2 h degradation reaction with BHET by Tcca and its variants. BHET were converted to TPA and MHET by biocatalysis. The total product release was quantified as the sum of the UV-detectable small molecules by high-performance liquid chromatography system (HPLC). Each measurement was conducted in triplicate, from which the average values \pm s.d. were calculated.

3. Discussion

Many PET plastic degrading enzymes originate from composting environments, such as LCC-cutinase [38] and PES-H1/H2 [39]. All these enzymes are thermophilic in nature, thereby exhibiting a high hydrolytic activity on polyester (e.g., PET) at high temperatures [17]. Thus, compost is a valuable source of thermophilic microorganisms and enzymes with polymer degrading activities. In this study, we verified that the polyester hydrolyzing activity of recombinant Tcca is a carboxylesterase from the compost-dwelling bacterium *Thermobacillus composti* KWC4. As most previously identified polyester hydrolases from compost samples are cutinase-like enzymes (EC 3.1.1.74), the PBAT depolymerizing activity of the carboxylesterase (EC 3.1.1.1) Tcca proved to be unusual.

Protein sequence analysis indicated that Tcca is similar to other carboxylesterases, with the conserved catalytic triad (serine, histidine, glutamate). Through SEM scanning, we observed some irregular grooves on PBAT film after Tcca treatment, suggesting that Tcca can hydrolyze the PBAT. PBAT degrading enzymes have been identified in both mesophilic

and thermophilic microorganisms. For example, Cbotu_EstA and Cbotu_EstB have an optimum temperature of 60 °C and 40 °C, respectively [20]. Pfl1 showed an optimum temperature of 50 °C [25], whereas Ple629 was most active at 30 °C [27]. The melting temperature (T_m) of Tcca reported in this research is 70 °C. The catalytic efficiency of Tcca is similar to known PABT degrading enzymes. After 24 h hydrolysis of PBAT plastic, the reaction catalyzed by WT Tcca produced about 4 μ M TPA per mole protein, while PpEst and Ple629 can produce 0.3 μ M TPA [21] and 60 μ M [27] TPA under similar conditions, respectively.

Based on structure modeling, we identified nine amino acid residues that should be involved in the binding polymer substrate. Therefore, we generated single site-specific variants to investigate their roles in the catalytic reaction, and we obtained Tcca variants with improved hydrolytic activities. Variant F325A has a 1.4-fold higher hydrolytic activity on PBAT film than WT. F325 is a bulky residue close to the catalytic triad (Figure 5C). PBAT has aliphatic moieties flanking the large aromatic TPA repeating units (Figure 5A). Hence, substituting the bulky F325 with smaller residues might provide more space to facilitate the entrance of polymeric substrate and thereby accelerate the degradation of PBAT. The variant E80A exhibits a 4.1-fold higher hydrolytic activity on BHET. E80 is located slightly further away from the suggested catalytic cavity (Figure 5C). In the homologous enzyme TfCa [39], the corresponding position has been identified as influencing the substrate binding. Therefore, we performed a similar residue substitution and hypothesized that the improved BHET hydrolysis activity of the Tcca E80A variant could also be a result of the less bulky alanine and modified charge. However, more detailed structural information is needed to verify the abovementioned hypothesis. Additionally, further protein engineering, such as combinatorial saturated mutagenesis, is needed to generate further better performing variants for both small molecule and polymeric substrates.

In conclusion, Tcca has a high potential for use in the biocatalytic recycling of commercial PBAT bioplastics as well as in the biodegradation of PET waste in order to serve as a helper enzyme to mitigate the product inhibition partly caused by BHET, similar to what has been described in recent studies [30,40]. Tcca could be further engineered to increase its thermal stability and hydrolytic activity in order to meet the requirements of potential applications at industrially relevant scales.

4. Materials and Methods

4.1. Materials

Terephthalic acid (TPA, CAS: 100–21–0) and bis-(2-hydroxyethyl) terephthalate (BHET, CAS: 956–26–2) and all other chemicals were purchased from Sigma–Aldrich (Shanghai, China), PBAT (CAS: 55231–08–8), and PBAT films were purchased from Shanghai Macklin Biochemical Co., Ltd (Shanghai, China).

4.2. Cloning and Site-Directed Mutagenesis

Tcca gene (GenBank accession number: WP_015255658.1) from *Thermobacillus composti* KWC4 was chemically synthesized by GENE ray Biotech Co. (Shanghai, China) and ligated into the pET–32a vector. Tcca mutants were prepared by using a QuickChange site-directed mutagenesis kit (Agilent Technologies, Santa Clara, CA, USA) with the pET32a–tcca plasmid as the template. The PCR products were incubated with DpnI (New England Biolabs, Hitchin, UK) to digest the original DNA template and then separately transformed into *Escherichia coli* strain XL1–Blue. The mutations were confirmed by sequencing; the sequences of the mutagenesis oligonucleotides are listed in Table 1.

4.3. Protein Purification

The pET32a–tcca plasmid was transformed into *E. coli* BL21(DE3) cells, which were grown in LB medium at 37 °C to an optical density (OD) 600 of 0.6–0.8 and then induced by 0.4 mM isopropyl β -D-thiogalactopyranoside (IPTG) at 16 °C for 20 h. Cells were harvested by centrifugation at 5000 \times g for 15 min and then re-suspended in lysis buffer

containing 25 mM Tris–HCl, pH 7.5, 150 mM NaCl and 20 mM imidazole, followed by disruption with a French Press. Cell debris were removed by centrifugation at $17,000\times g$ for 1 h. The supernatant was then applied to a Ni–NTA column with FPLC system ((Åkta purifier, GE Healthcare, Chicago, IL, USA). The target proteins were eluted at ~100 mM imidazole while using a 20–250 mM imidazole gradient. Each protein was dialyzed against a buffer containing 25 mM Tris–HCl, pH 7.5, 150 mM NaCl, and was subjected to TEV protease digestion overnight to remove the $6\times$ His tag. The mixture was then passed through another Ni–NTA column. The untagged protein was eluted with 25 mM Tris–HCl, pH 7.5, 150 mM NaCl. The purity of each protein (>95%) was checked by SDS–PAGE analysis. The purified proteins were each concentrated to 10 mg/mL for the following usage.

Table 1. Oligonucleotides used for mutagenesis.

Residue Substitutions	Sequence (5'–3')
Y77W	ATTGATGTTAATAATATT tgg ACCCGCGAATGGGCCGTG
R79A	GTAAATAATATTTATACCgctGAATGGGCGGTGGACCCG
E80A	AATAATATTTATACCCGCGctTGGGCCGTGGACCCGGAT
W81A	AATATTTATACCCGCGAAgctGCCGTGGACCCGGATATT
E129A	CAGGTGGGTCATGCAAGTgctATGGAATTTGATGGCGAA
F130A	CATGCAAGTGAAATGGAAgctGATGGCGAACGCATTGCA
F325A	GGTAATACCACCGATGAAgctATTAGTCGTCCGCAGGTT
K427A	TTTTTTGAAACCTTAGCCgctTGTGGCGCCCCGTTTGTG
W429A	GAAACCTTAGCCAAATGTgctCGCCCCGTTTGTGGCGAAA

4.4. Characterization of Melting Temperature, Optimal pH and Temperature of Tcca

The melting temperatures (T_m) of Tcca and its variants were determined using the nano–differential scanning calorimeter (DSC, TA Instruments, New Castle County, DE, USA), and the purified proteins were diluted to 1.0 mg/mL (PBS buffer, pH 7.4) and degassed immediately prior to DSC testing. Samples were heated from 10 to 80 °C at a rate of 1 °C per minute during the measurement; the basal line value of buffer without protein was removed from the protein trace.

The optimum pH range of Tcca was tested in buffers ranging from pH 6.0 to 9.5 (pH 6.0–7.0: 0.1 M $\text{Na}_2\text{HPO}_4/\text{NaH}_2\text{PO}_4$ buffer, pH 7.0–8.0: 0.1 M $\text{K}_2\text{HPO}_4/\text{KH}_2\text{PO}_4$ buffer, pH 8.0–9.0: 0.1 M Tris–HCl buffer, pH 9.0–9.5: 0.1 M glycine–NaOH buffer). All the reactions were performed with a piece of PBAT film ($\text{Ø}8\text{ mm} \times 8\text{ mm}$ square) with 10.9 μM enzyme in 0.8 mL buffer at 300 rpm, 40 °C for 24 h. The optimum temperature range of Tcca was measured in the range of 30 to 70 °C. All the reactions were performed with a piece of PBAT film ($\text{Ø}8\text{ mm} \times 8\text{ mm}$ square) with 10.9 μM enzyme in 0.8 mL buffer containing 100 mM PBS (pH 8.0) at 300 rpm for 24 h.

4.5. Scanning Electron Microscopy

After enzymatic treatment, PBAT films were first washed with distilled water and ethanol. The morphology of PBAT films before and after enzyme treatment was examined by SU8010 SEM (Hitachi, Tokyo, Japan) at an accelerating voltage of 1.0 kV. Samples were sputter–coated with platinum in an ion sputter (E1045, Hitachi, Japan).

4.6. Hydrolysis Activity of PBAT and BHET by Tcca and Its Mutants

PBAT films with a size of 8 mm \times 8 mm were used for the hydrolysis experiments. Prior to incubation, the films were washed with Milli–Q water three times and dried. The films ($\text{Ø}8\text{ mm}$) were soaked with 10.9 μM enzyme in 0.8 mL buffer containing 100 mM PBS (pH 8.0) at 300 rpm, 40 °C. The reactions were terminated after 24 h by dilution with the same volume of cold methanol. The supernatant obtained by centrifugation ($15,000\times g$, 10 min) was then analyzed by HPLC. After filtration through a 0.22 μm filter membrane, 10 μL of assay solution was analyzed using a HPLC system (Agilent 1200, Agilent Technologies, Wilmington, DE, USA) equipped with a Welch Ultimate XB–C18

column (4.6 × 250 mm, 5 µm, Welch Materials, Inc., Shanghai, China). The mobile phase for PBAT hydrolysates was acetonitrile with 0.1% (V/V) formic acid in Milli-Q water at a flow rate of 0.8 mL/min, and the effluent was monitored at a wavelength of 240 nm. The typical elution condition was 0–9 min with 25% acetonitrile, 9–10 min with 25–55% acetonitrile linear gradient, and 10–20 min with 55% acetonitrile. The hydrolytic product TPA was identified by comparing the retention time with the standard compound, and reactions without enzyme were used as negative controls.

Activity assays of Tcca and its mutants for BHET hydrolysis were performed in 20% DMSO in 100 mM PBS (pH 8.0) and 1.0 mM BHET at 40 °C, the final concentration of Tcca was 10.9 µM, and the reaction volume was 0.8 mL. The supernatant obtained by centrifugation (15,000 × g, 10 min) was then analyzed by HPLC using the same machine and column as for PBAT activity detections. The mobile phase for BHET reactions was 19% acetonitrile with 0.1% (V/V) formic acid in Milli-Q water at a flow rate of 0.8 mL/min, and the effluent was monitored at a wavelength of 254 nm. The hydrolytic products of TPA and MHET were identified by comparing the retention time with those of the standard compounds. All samples were analyzed in triplicate in each independent experiment; the resulting data were averaged, and the standard errors were calculated.

Author Contributions: R.W., Q.G., W.L. and X.H. conceived this research; P.W., Z.L., J.G., Y.Z., H.W. and H.Q. expressed and purified protein, and conducted enzyme characterization, SEM and DSC analysis, and data analysis; R.W., W.L. and X.H. wrote the paper. All authors have read and agreed to the published version of the manuscript.

Funding: This research was funded by the National Key Research and Development Program of China (2021YFA0910200) and Tianjin Synthetic Biotechnology Innovation Capacity Improvement Project (TSBICIP–PTJJ–008, TSBICIP–IJCP–003, TSBICIP–KJGG–009–01, TSBICIP–KJGG–002–06). R.W. acknowledges the financial support of the MixUp project, which has received funding from the European Union’s Horizon 2020 research and innovation program under grant agreement no. 870294.

Data Availability Statement: All datasets presented in this study are included in the article.

Acknowledgments: The authors acknowledge Jie Zhang at the Laboratory of Structural Biology (TIB, CAS) for technical help with DSC.

Conflicts of Interest: The authors declare no conflict of interest.

References

1. Witt, U.; Yamamoto, M.; Seeliger, U.; Muller, R.J.; Warzelhan, V. Biodegradable polymeric materials—not the origin but the chemical structure determines biodegradability. *Angew. Chem. Int. Ed.* **1999**, *38*, 1438–1442. [[CrossRef](#)]
2. Gupta, A.; Chudasama, B.; Chang, B.P.; Mekonnen, T. Robust and sustainable PBAT–Hemp residue biocomposites: Reactive extrusion compatibilization and fabrication. *Compos. Sci. Technol.* **2021**, *215*, 109014. [[CrossRef](#)]
3. Jiang, L.; Wolcott, M.P.; Zhang, J. Study of biodegradable Poly(lactide)/Poly(butylene adipate–co–terephthalate) blends. *Biomacromolecules* **2006**, *7*, 199–207. [[CrossRef](#)]
4. Pinheiro, I.F.; Ferreira, F.V.; Souza, D.H.S.; Gouveia, R.F.; Lona, L.M.F.; Morales, A.R.; Mei, L.H.I. Mechanical, rheological and degradation properties of PBAT nanocomposites reinforced by functionalized cellulose nanocrystals. *Eur. Polym. J.* **2017**, *97*, 356–365. [[CrossRef](#)]
5. Pavon, C.; Aldas, M.; de la Rosa–Ramirez, H.; Lopez–Martinez, J.; Arrieta, M.P. Improvement of PBAT processability and mechanical performance by blending with pine resin derivatives for injection moulding rigid packaging with enhanced hydrophobicity. *Polymers* **2020**, *12*, 2891. [[CrossRef](#)] [[PubMed](#)]
6. Pal, A.K.; Wu, F.; Misra, M.; Mohanty, A.K. Reactive extrusion of sustainable PHBV/PBAT–based nanocomposite films with organically modified nanoclay for packaging applications: Compression moulding vs. cast film extrusion. *Compos. Part B Eng.* **2020**, *198*, 108141. [[CrossRef](#)]
7. Pagno, V.; Modenes, A.N.; Dragunski, D.C.; Fiorentin–Ferrari, L.D.; Caetano, J.; Guellis, C.; Goncalves, B.C.; dos Anjos, E.V.; Pagno, F.; Martinelli, V. Heat treatment of polymeric PBAT/PCL membranes containing activated carbon from Brazil nutshell biomass obtained by electrospinning and applied in drug removal. *J. Environ. Chem. Eng.* **2020**, *8*, 104159. [[CrossRef](#)]
8. Oguz, H.; Dogan, C.; Kara, D.; Ozen, Z.T.; Ovali, D.; Nofar, M. Development of PLA–PBAT and PLA–PBSA bio–blends: Effects of processing type and PLA crystallinity on morphology and mechanical properties. In Proceedings of the Europe/Africa Conference Dresden 2017—Polymer Processing Society PPS, Online, 27–29 June 2019; Volume 2055. [[CrossRef](#)]

9. Nunes, F.C.; Ribeiro, K.C.; Martini, F.A.; Barrioni, B.R.; Santos, J.P.F.; Carvalho, B.M. PBAT/PLA/cellulose nanocrystals bio-composites compatibilized with polyethylene grafted maleic anhydride (PE-g-MA). *J. Appl. Polym. Sci.* **2021**, *138*, 51342. [[CrossRef](#)]
10. Nobile, M.R.; Crocitti, A.; Malinconico, M.; Santagata, G.; Cerruti, P. Preparation and characterization of polybutylene succinate (PBS) and polybutylene adipate-terephthalate (PBAT) biodegradable blends. In Proceedings of the 9th International Conference on Times of Polymers and Composites: From Aerospace to Nanotechnology, Ischia, Italy, 17–21 June 2018; Volume 1981. [[CrossRef](#)]
11. Pietrosanto, A.; Scarfato, P.; Di Maio, L.; Incarnato, L. Development of eco-sustainable PBAT-based blown films and performance analysis for food packaging applications. *Materials* **2020**, *13*, 5395. [[CrossRef](#)]
12. Gambarini, V.; Pantos, O.; Kingsbury, J.M.; Weaver, L.; Handley, K.M.; Lear, G. Phylogenetic distribution of plastic-degrading microorganisms. *mSystems* **2021**, *6*, e01112-20. [[CrossRef](#)]
13. Kanwal, A.; Zhang, M.; Sharaf, F.; Li, C.T. Screening and characterization of novel lipase producing *Bacillus* species from agricultural soil with high hydrolytic activity against PBAT poly (butylene adipate co terephthalate) co-polyesters. *Polym. Bull.* **2022**, *79*, 10053–10076. [[CrossRef](#)]
14. Kanwal, A.; Zhang, M.; Sharaf, F.; Li, C.T. Polymer pollution and its solutions with special emphasis on Poly (butylene adipate terephthalate (PBAT)). *Polym. Bull.* **2022**, *79*, 9303–9330. [[CrossRef](#)]
15. Qi, X.; Ren, Y.; Wang, X. New advances in the biodegradation of Poly(lactic) acid. *Int. Biodeterior. Biodegrad.* **2017**, *117*, 215–223. [[CrossRef](#)]
16. Marten, E.; Muller, R.J.; Deckwer, W.D. Studies on the enzymatic hydrolysis of polyesters. II. Aliphatic-aromatic copolyesters. *Polym. Degrad. Stab.* **2005**, *88*, 371–381. [[CrossRef](#)]
17. Wei, R.; von Haugwitz, G.; Pfaff, L.; Mican, J.; Badenhorst, C.P.S.; Liu, W.; Weber, G.; Austin, H.P.; Bednar, D.; Damborsky, J.; et al. Mechanism-based design of efficient PET hydrolases. *ACS Catal.* **2022**, *12*, 3382–3396. [[CrossRef](#)]
18. Tokiwa, Y.; Suzuki, T. Hydrolysis of polyesters by lipases. *Nature* **1977**, *270*, 76–78. [[CrossRef](#)]
19. Herrero Acero, E.; Ribitsch, D.; Steinkellner, G.; Gruber, K.; Greimel, K.; Eiteljoerg, I.; Trotscha, E.; Wei, R.; Zimmermann, W.; Zinn, M.; et al. Enzymatic Surface Hydrolysis of PET: Effect of Structural Diversity on Kinetic Properties of Cutinases from *Thermobifida*. *Macromolecules* **2011**, *44*, 4632–4640. [[CrossRef](#)]
20. Perz, V.; Baumschlager, A.; Bleymaier, K.; Zitzenbacher, S.; Hromic, A.; Steinkellner, G.; Pairitsch, A.; Lyskowski, A.; Gruber, K.; Sinkel, C.; et al. Hydrolysis of synthetic polyesters by *Clostridium botulinum* esterases. *Biotechnol. Bioeng.* **2016**, *113*, 1024–1034. [[CrossRef](#)]
21. Wallace, P.W.; Haernvall, K.; Ribitsch, D.; Zitzenbacher, S.; Schittmayer, M.; Steinkellner, G.; Gruber, K.; Guebitz, G.M.; Birner-Gruenberger, R. PpEst is a novel PBAT degrading polyesterase identified by proteomic screening of *Pseudomonas pseudoalcaligenes*. *Appl. Microbiol. Biotechnol.* **2017**, *101*, 2291–2303. [[CrossRef](#)]
22. Kitadokoro, K.; Thumarat, U.; Nakamura, R.; Nishimura, K.; Karatani, H.; Suzuki, H.; Kawai, F. Crystal structure of cutinase Est119 from *Thermobifida alba* AHK119 that can degrade modified polyethylene terephthalate at 1.76Å resolution. *Polym. Degrad. Stab.* **2012**, *97*, 771–775. [[CrossRef](#)]
23. Perz, V.; Bleymaier, K.; Sinkel, C.; Kueper, U.; Bonnekessel, M.; Ribitsch, D.; Guebitz, G.M. Substrate specificities of cutinases on aliphatic-aromatic polyesters and on their model substrates. *New Biotechnol.* **2016**, *33*, 295–304. [[CrossRef](#)] [[PubMed](#)]
24. Kukolya, J. *Thermobifida cellulolytica* sp. nov., a novel lignocellulose-decomposing actinomycete. *Int. J. Syst. Evol. Microbiol.* **2002**, *52*, 1193–1199. [[CrossRef](#)] [[PubMed](#)]
25. Biundo, A.; Hromic, A.; Pavkov-Keller, T.; Gruber, K.; Quartinello, F.; Haernvall, K.; Perz, V.; Arrell, M.S.; Zinn, M.; Ribitsch, D.; et al. Characterization of a poly(butylene adipate-co-terephthalate)-hydrolyzing lipase from *Pelosinus fermentans*. *Appl. Microbiol. Biotechnol.* **2016**, *100*, 1753–1764. [[CrossRef](#)]
26. Kleeberg, I.; Welzel, K.; VandenHeuvel, J.; Müller, R.J.; Deckwer, W.D. Characterization of a new extracellular hydrolase from *Thermobifida fusca* degrading aliphatic-aromatic copolyesters. *Biomacromolecules* **2005**, *6*, 262–270. [[CrossRef](#)] [[PubMed](#)]
27. Meyer Cifuentes, I.E.; Wu, P.; Zhao, Y.; Liu, W.; Neumann-Schaal, M.; Pfaff, L.; Barys, J.; Li, Z.; Gao, J.; Han, X.; et al. Molecular and biochemical differences of the tandem and cold-adapted PET hydrolases Ple628 and Ple629, isolated from a marine microbial consortium. *Front. Bioeng. Biotechnol.* **2022**, *10*, 930140. [[CrossRef](#)] [[PubMed](#)]
28. Li, Z.; Zhao, Y.; Wu, P.; Wang, H.; Li, Q.; Gao, J.; Qin, H.M.; Wei, H.; Bornscheuer, U.T.; Han, X.; et al. Structural insight and engineering of a plastic degrading hydrolase Ple629. *Biochem. Biophys. Res. Commun.* **2022**, *626*, 100–106. [[CrossRef](#)] [[PubMed](#)]
29. Satti, S.M.; Shah, A.A. Polyester-based biodegradable plastics: An approach towards sustainable development. *Letts. Appl. Microbiol.* **2020**, *70*, 413–430. [[CrossRef](#)]
30. Jochens, H.; Aerts, D.; Bornscheuer, U.T. Thermostabilization of an esterase by alignment-guided focussed directed evolution. *Protein Eng. Des. Sel.* **2010**, *23*, 903–909. [[CrossRef](#)]
31. Carr, P.D.; Ollis, D.L. Alpha/beta hydrolase fold: An update. *Protein Pept. Lett.* **2009**, *16*, 1137–1148. [[CrossRef](#)]
32. von Haugwitz, G.; Han, X.; Pfaff, L.; Li, Q.; Wei, H.; Gao, J.; Methling, K.; Ao, Y.; Brack, Y.; Mican, J.; et al. Structural insights into (Tere)phthalate-ester hydrolysis by a carboxylesterase and its role in promoting PET depolymerization. *ACS Catal.* **2022**, *12*, 15259–15270. [[CrossRef](#)]
33. Liu, P.; Ewis, H.E.; Tai, P.C.; Lu, C.D.; Weber, I.T. Crystal structure of the *Geobacillus stearothermophilus* carboxylesterase Est55 and its activation of prodrug CPT-11. *J. Mol. Biol.* **2007**, *367*, 212–223. [[CrossRef](#)] [[PubMed](#)]

34. Spiller, B.; Gershenson, A.; Arnold, F.H.; Stevens, R.C. A structural view of evolutionary divergence. *Proc. Natl. Acad. Sci. USA* **1999**, *96*, 12305–12310. [[CrossRef](#)]
35. Jumper, J.; Evans, R.; Pritzel, A.; Green, T.; Figurnov, M.; Ronneberger, O.; Tunyasuvunakool, K.; Bates, R.; Zidek, A.; Potapenko, A.; et al. Highly accurate protein structure prediction with AlphaFold. *Nature* **2021**, *596*, 583–589. [[CrossRef](#)] [[PubMed](#)]
36. Saini, P.; Grewall, A.; Hooda, S. In silico approach for identification of polyethylene terephthalate hydrolase (PETase)-like enzymes. *Bioremediat. J.* **2022**. [[CrossRef](#)]
37. Denesyuk, A.; Dimitriou, P.S.; Johnson, M.S.; Nakayama, T.; Denessiouk, K. The acid–base–nucleophile catalytic triad in ABH-fold enzymes is coordinated by a set of structural elements. *PLoS ONE* **2020**, *15*, e0229376. [[CrossRef](#)] [[PubMed](#)]
38. Sulaiman, S.; Yamato, S.; Kanaya, E.; Kim, J.J.; Koga, Y.; Takano, K.; Kanaya, S. Isolation of a novel cutinase homolog with polyethylene terephthalate-degrading activity from leaf-branch compost by using a metagenomic approach. *Appl. Environ. Microbiol.* **2012**, *78*, 1556–1562. [[CrossRef](#)] [[PubMed](#)]
39. Pfaff, L.; Gao, J.; Li, Z.; Jäckering, A.; Weber, G.; Mican, J.; Chen, Y.; Dong, W.; Han, X.; Feiler, C.G.; et al. Multiple substrate binding mode-guided engineering of a thermophilic PET hydrolase. *ACS Catal.* **2022**, *12*, 9790–9800. [[CrossRef](#)]
40. Tarazona, N.A.; Wei, R.; Brott, S.; Pfaff, L.; Bornscheuer, U.T.; Lendlein, A.; Machatschek, R. Rapid depolymerization of poly(ethylene terephthalate) thin films by a dual-enzyme system and its impact on material properties. *Chem. Catal.* **2022**, *2*, 3573–3589. [[CrossRef](#)]

Disclaimer/Publisher’s Note: The statements, opinions and data contained in all publications are solely those of the individual author(s) and contributor(s) and not of MDPI and/or the editor(s). MDPI and/or the editor(s) disclaim responsibility for any injury to people or property resulting from any ideas, methods, instructions or products referred to in the content.